An Implicit Finite Element Structural Dynamic Formulation for Long-Duration Accidents in Reactor Piping Systems

C.Y. Wang

Argonne National Laboratory, Reactor Analysis and Safety Division, 9700 South Cass Ave., Argonne, Illinois 60439, U.S.A.

Abstract

This paper describes an implicit three-dimensional finite-element formulation for the structural analysis of reactor-piping system. The numerical algorithm considers hoop, flexural, axial, and torsion modes of the piping structures. It is unconditionally stable and can be used for calculation of piping response under static or long-duration dynamic loads.

The method uses a predictor-corrector, successive iterative scheme which satisfies the equilibrium equations. A set of stiffness equations representing the discretized equations of motion are derived to predict the displacement increments. The calculated displacement increments are then used to correct the element nodal forces. The algorithm is fairly general, and is capable of treating large displacements and elastic-plastic materials with thermal and strain-rate effects.

1. Introduction

Maintaining the structural integrity of the piping system of Liquid Metal Fast Breeder Reactors (LMFBRs) is essential to the safe operation of the reactor and steam-supply systems. In a safety analysis various transient loads can be imposed on the piping systems, including: (1) hydrodynamic loading resulting from pressure-wave propagation due to a hypothetical core-disruptive accident (HCDA) or a sodium-water reactor (SWR); (2) thermal loading generated by hot coolant suddenly entering the piping system; (3) structural loads due to seismic events; and (4) loads encountered during normal reactor operations such as internal pressurization, thermal effects, and creep phenomena.

Since 1975 substantial research efforts have been devoted to the development of numerical techniques and computer programs for analyzing pressure-wave transients in reactor-piping systems. At ANL a three-dimensional piping code, called SHAPS [1-4], has been developed. It uses an implicit time-integration scheme for the hydrodynamic analysis together with an explicit time-integration scheme for the structural calculation. The code is very efficient for short-duration problems involving rapid fluid transient. However, for static or long-duration dynamic problems, it becomes prohibitively expansive because of its restricted small time steps associated with the explicit structural integration scheme.

In order to apply the SHAPS code to transient conditions with longer solution times, an optional program module, PIPE3D-IMP, which uses the implicit time integration for the structural analysis has been developed. This implicit program is unconditionally stable and can be used for long-duration calculations of piping response under static or quasi-dynamic loads. Presently, this program consists of only a pipe element with eight degrees of freedom per node, i.e. three displacements, three rotations, one membrane displacement, and one bending rotation. This implicit three-dimensional pipe element can be used to model straight pipes, elbows, and inline components. We will proceed to describe the analytical development and illustrative examples.

2. Analytical Development

2.1 Stiffness Matrix

As a first step, we shall develop the stiffness matrix of a 3-D pipe element that considers both hoop and flexural stresses, including bending in both planes. Figure 1 shows a typical element of length ℓ. The $\hat{x}$, $\hat{y}$, and $\hat{z}$ coordinates are the co-rotational coordinates associated with the element. The x, y, and z coordinates are the global coordinates. First, we wish to develop a constant element stiffness matrix $[\hat{K}_e]$ so that in the co-rotational coordinate system we have

$$\{f'\} = [\hat{K}_e]\{d'\} \quad \text{or} \quad \{\Delta f'\} = [\hat{K}_e]\{\Delta d'\} \quad . \tag{1}$$

using principle of virtue work, one can show that

$$\{f'\} = \left(\int_V [B']^T [C'] [B'] \, dV\right) \{d'\} = [\hat{K}_e] \{d'\} \quad , \tag{2}$$

where

$$[\hat{K}_e] = \int_V [B']^T [C'] [B'] \, dV \quad , \tag{3}$$

is the element stiffness matrix written in the convective coordinate system; [C'] is the material matrix; [B'] relates the displacements to the strains.

By definition, the [B'] matrix has the form

$$[B'] = [\underset{\sim}{B}_1, \underset{\sim}{B}_2] \quad , \tag{4}$$

where

$$[B'_I] = \begin{bmatrix} \frac{(-1)^I}{\ell} & -\hat{y}\psi_{I,xx} & -\hat{z}\psi_{I,xx} & 0 & \hat{z}\phi_{I,xx} & -\hat{y}\phi_{I,xx} & -\eta\psi_{I,xx} & -\eta\phi_{I,xx} \\ 0 & 0 & 0 & 0 & 0 & 0 & \psi_I/r & \phi_I/r \\ 0 & 0 & 0 & (-1)^I \frac{r}{\ell} & 0 & 0 & 0 & 0 \end{bmatrix} \tag{5}$$

In eq. (5) ψ and ϕ are the shape functions [1], r is the radial coordinate, and prime denotes partial differentiation.

2.2 Temporal Integration

For the convenience of developing the implicit-integration algorithm, let us rewrite the global equations of motion in the form

$$[M]\ \{a_{n+1}\} + \{F^{int}(d_{n+1})\} = \{F^{ext}\} \quad , \tag{6}$$

where, understandably, $[M]$, $\{a\}$, $\{F^{int}\}$, and $\{F^{ext}\}$ denote the global mass matrix, nodal accelerations, nodal internal and external forces, respectively. The subscript n+1 denotes the advanced-time step. Thus, subscript n used subsequently will denote the previous time cycle. Also, we should mention that the internal force $\{F^{int}\}$ is a function of nodal displacements in the advanced-time cycle.

Furthermore, let us assume that

$$\{d^{i+1}_{n+1}\} = \{d^{i}_{n+1}\} + \{\Delta d\} \quad , \tag{7}$$

where superscripts i+1 and i denote the advanced and previous iteration, respectively.

The equations of motion can then be integrated in time by an implicit algorithm based on the Newmark-β difference formulas,

$$\{a_{n+1}\} = [\{d_{n+1}\} - \{d_n\} - \Delta t\ \{v_n\} - (½ - \beta)\ \Delta t^2\ \{a_n\}]/\beta\Delta t^2 \quad . \tag{8}$$

The nodal accelerations and velocities corresponding to the advanced iteration can be written as

$$\{a^{i+1}_{n+1}\} = [\{d^{i}_{n+1}\} + \{\Delta d\} - \{d_n\} - \Delta t\ \{v_n\} - (½ - \beta)\ \Delta t^2\ \{a_n\}]/\beta\Delta t^2 \tag{9}$$

and

$$\{v^{i+1}_{n+1}\} = \{v_n\} + (1 - \gamma)\ \Delta t\ \{a_n\} + \gamma\Delta t\ \{a^{i+1}_{n+1}\} \quad . \tag{10}$$

In eqs. (8-10), β and γ are the integration constants. Based on the method of linearization, the nodal internal force at the advanced-time iteration can be expressed as a function of previous iteration values, or

$$\{F^{int}(d^{i+1}_{n+1}\} \simeq \{F^{int}(d^{i}_{n+1})\} + [K(d^{i}_{n+1})]\ \{\Delta d\} + \ldots . \tag{11}$$

Substituting eqs. (9) and (11) into eq. (6), and after some rearranging we have

$$[K^*]\ \{\Delta d\} = \{\Delta F^*\} \quad , \tag{12}$$

where

$$[K^*] = [M] + \beta\Delta t^2 \; [K(d^i_{n+1})] \quad , \tag{13}$$

and

$$\{\Delta F^*\} = \beta\Delta t^2 \; [F^{ext}_{n+1} - F^{int}(d^i_{n+1})]$$

$$- [M] \left[\{d^i_{n+1}\} - \{d_n\} - \Delta t \; \{v_n\} - (\tfrac{1}{2} - \beta) \; \Delta t^2 \; \{a_n\} \right] \quad . \tag{14}$$

Equation (12) is solved iteratively at each time step to obtain the displacement increment $\{\Delta d\}$. The new displacements, accelerations, and velocities are then found from eqs. (7), (9), and (10).

3. Results

3.1 Transverse Displacements of a Cantilever Pipe

To evaluate the performance of the implicit scheme, the program was applied to the cantilever pipe shown in Fig. 2. A calculation was carried out by applying a Y-direction shear load at the free end. In this loading condition both static and dynamic cases were considered. The computed displacements are compared with the theoretical results.

Figure 3 shows the calculated results on the deflections of the tip of the cantilever pipe. As can be seen, the dynamic deflections oscillated about the static elastic deflection. The periods of oscillation, corresponding to shear load in the Y direction, was in very good agreement with the theoretical values obtained from the simple beam theory.

3.2 Response of a Three-Dimensional Pipe-Elbow Loop

To further test the performance of the implicit structural module, a sample problem which couples different modes of deformation and also demonstrated the capability of modeling elbows through the implicit time-integration is presented. This pipe system consists of three pipes connected through two 90° elbows as shown in Fig. 4. All pipes and elbows have the same cross-section dimensions of 3.81-cm inside radius and 0.33-cm-thick walls. Each elbow is represented by five pipe elements.

A point load parallel to the global X-axis is applied at the midpoint of the second pipe as shown in Fig. 4. The load is increased linearly from zero to 2000 N in 50 μs and then held constant. The problem was run using both the implicit and explicit time-integration schemes of SHAPS, and the solutions were compared with those obtained from SAP-IV and WHAMS [6,7]. Referring to Fig. 4, one can see that pipe 1 is subject to axial and bending loadings, pipe 2 is subject to bending loading, and pipe 3 is subject to bending and torsional loadings.

Excellent agreement among all solutions was obtained at all five locations, i.e., at nodes 9, 20, 33, 47, and 57. Examples of such comparisons are shown in Figs. 5, 6, and 7. Figure 5 shows the Y-displacement history at node 9 of pipe 1. Figure 6 shows the X-displacement history at node 33 where the load is applied, and Fig. 7 shows the Z-rotational history at node 47 of elbow 2, which represents the twisting rotation at that node.

4. Acknowledgments

This work was performed in the Engineering Mechanics Program of the Reactor Analysis and Safety Division at Argonne National Laboratory, under the auspices of the U.S. Department of Energy.

References

[1] A-MONEIM, M. T., CHANG, Y. W., BELYTSCHKO, T. B., "Three-dimensional Response of Piping Systems to Internally Propagating Pressure Pulses," Trans. 5th Int. Conf. on Structural Mechanics in Reactor Technology, Paper E 3/3, Vol. E, Berlin, Germany (August, 1979).

[2] WANG, C. Y., A-MONEIM, M. T., BELYTSCHKO, T. B., "Integrated Analysis of Piping Systems," Trans. 6th Int. Conf. on Structural Mechanics in Reactor Technology, Paper E 6/1, Paris (August, 1981).

[3] WANG, C. Y., "A Three-Dimensional Method for Integrated Transient Analysis of Reactor-Piping Systems," Nuclear Engineering and Design, Vol. 68, No. 2, pp. 175-184 (March, 1982).

[4] WANG, C. Y., "Theory and Application of a Three-Dimensional Code SHAPS to Complex Piping Systems," Advances in Fluid-Structure Interaction, The 4th Nat. Congress on Pressure Vessel Piping Technology, ASME pvp-75, Book No. H00261, pp. 139-157, Portland, OR (June, 1983).

[5] BELYTSCHKO, T. B., SHWER, B., KLEIN, M. J., "Large Displacement, Transient Analysis of Space Frames," Int. J. of Numerical Methods in Engineering, Vol. 11, p. 65 (1977).

[6] BATHE, K. J., et al., "SAP-IV: A Structural Analysis Program for Static and Dynamic Response of Linear Systems," EERC 73-11, University of California (June, 1973).

[7] BELYTSCHKO, T. B., TSAY, C. S., "WHAMSE: Program for Three-Dimensional Nonlinear Structural Dynamics," EPRI Report NP-2250 (February, 1982).

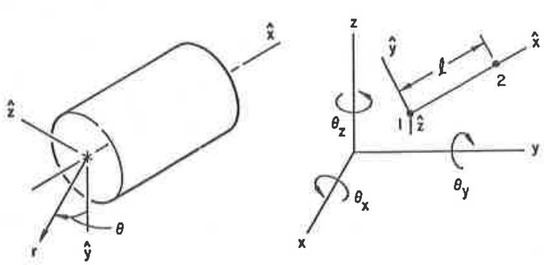

Fig. 1. Generic Pipe Element and Element Coordinates

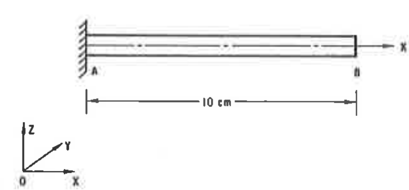

Fig. 2. Configuration of a Cantilever Pipe

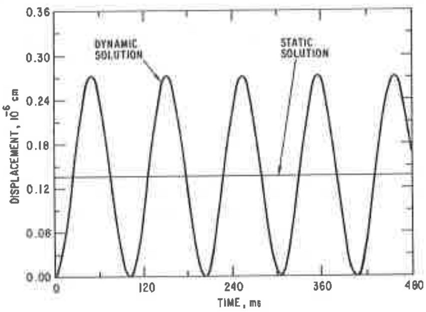

Fig. 3. The Y-Displacement Time History at the Free End of the Cantilever Pipe

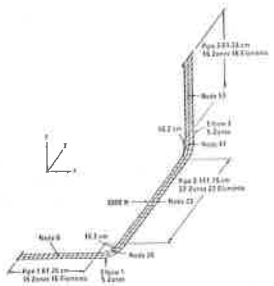

Fig. 4. Model of the Three-Dimensional Piping System

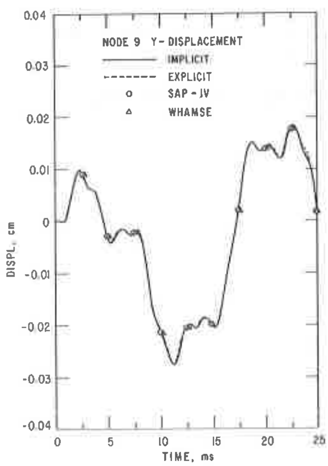

Fig. 5. The Y-Displacement Time History at Node 9 of Pipe 1

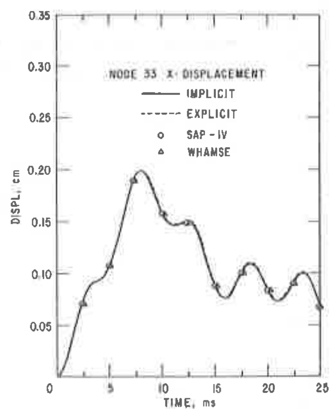

Fig. 6. The X-Displacement Time History at Node 33 of Pipe 2

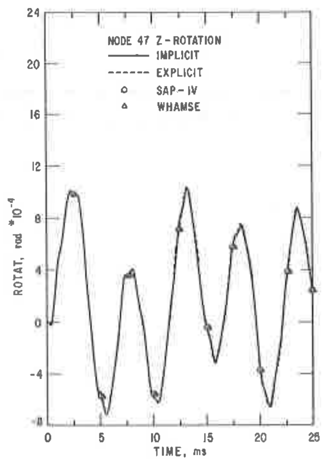

Fig. 7. The Z-Rotation Time History at Node 47 of Elbow 2